



NRL/MR/5652--08-9137

Field Test on the Feasibility of Remoting HF Antenna with Fiber Optics

VINCENT J. URICK
ALEX HASTINGS
JAMES L. DEXTER
KEITH J. WILLIAMS

*Photonics Technology Branch
Optical Sciences Division*

CHRISTOPHER SUNDERMAN
JOHN DIEHL
KRISTINA COLLADAY
*SFA, Inc.
Crofton, Maryland*

July 31, 2008

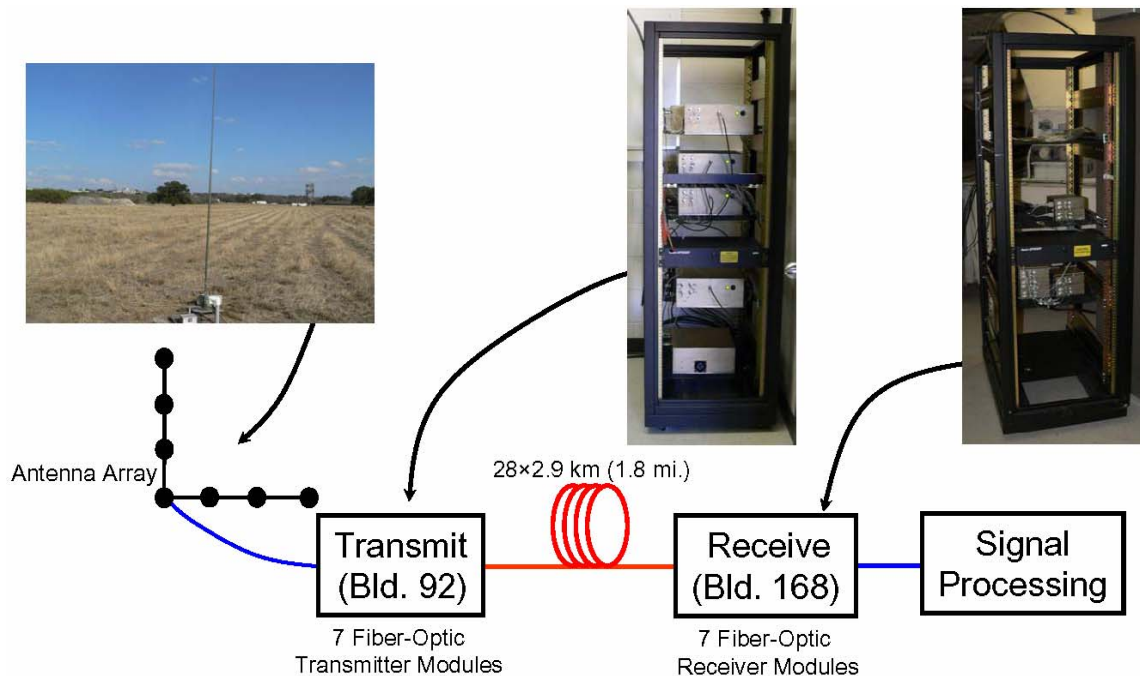
TABLE OF CONTENTS

EXECUTIVE SUMMARY.....	1
1 INTRODUCTION.....	2
2 LINK DESIGN.....	3
3 PREPARATION AND INSTALLATION.....	5
4 HF PERFORMANCE.....	9
5 SUMMARY AND CONCLUSIONS.....	12
ACKNOWLEDGEMENTS.....	12
REFERENCES.....	13
APPENDIX I: BASIC OPERATING INSTRUCTIONS.....	15
APPENDIX II: PARTS LIST.....	16

FIELD TEST ON THE FEASIBILITY OF REMOTING HF ANTENNA WITH FIBER OPTICS

EXECUTIVE SUMMARY

This report details the results of a field test carried out 19-22 February 2008 at the Southwest Research Institute (SwRI), San Antonio, Texas, where a 2.9-km (1.8-mile) fiber-optic link was employed to remote a high-frequency (HF, 2-30 MHz) direction-finding (DF) array. As shown below, the test link comprised a seven-element “L” array connected to seven fiber-optic transmitter modules, the 2.9-km fiber run, and seven fiber-optic receiver modules. The outputs of the fiber-optic receivers were fed to a signal-processing suite. It must be noted that while the test at SwRI was at 2.9 km, the fiber-optic link yields the same performance up to a 7-km transmission distance. The complete details of the design and laboratory performance of the fiber-optic link are provided in [1]: V. J. Urick, et al., “Analysis of fiber-optic links for HF antenna remoting,” NRL Memorandum Report, NRL/MR/5650-08-9101, Mar. 2008. This present report concentrates on the results of the field test, namely, that 1) *The measured field data agree with the previous theoretical analysis and experimental laboratory results for the fiber-optic link* and 2) *The measured system performance in the field indicates that HF antenna remoting up to 7 km (4.4 miles) is feasible with the fiber-optic link*. The units will remain at SwRI for testing in addition to that described in this report.



Field-Test Architecture

Shown are photographs of the antenna field, the fiber-optic transmitters and the fiber-optic receivers. In the block diagram, blue designates the electrical paths and red designates the optical path.

FIELD TEST ON THE FEASIBILITY OF REMOTING HF ANTENNA WITH FIBER OPTICS

1 INTRODUCTION

In this document we report on a field test of an analog fiber-optic link for the remoting of an array of high-frequency (HF, 2-30 MHz) antennas. The field test took place 19-22 February 2008 using the facilities at Southwest Research Institute (SwRI), Signal Exploitation and Geolocation Division, San Antonio, Texas. As shown with a general block diagram in Figure 1, the test bed comprises a seven-element antenna array electronically connected to seven fiber-optic transmitters, which are optically connected to seven optical receivers. The electronic output of the fiber optic link is then connected to signal-processing equipment. The optical transmission distance is 2.9 km but as described in [1], the fiber optic link will provide the same performance at a distance ≤ 7 km. A thorough description of the test bed and the successful field test results will be given in this report.

The report is organized into four additional sections. The link architecture is reviewed in Section 2, noting that the link design is detailed thoroughly in a previous accompanying report [1]. In Section 3, the steps taken to install the fiber-optic link in the field are described. The measured performance in the field is given in Section 4 and a summary with conclusions is provided in Section 5.

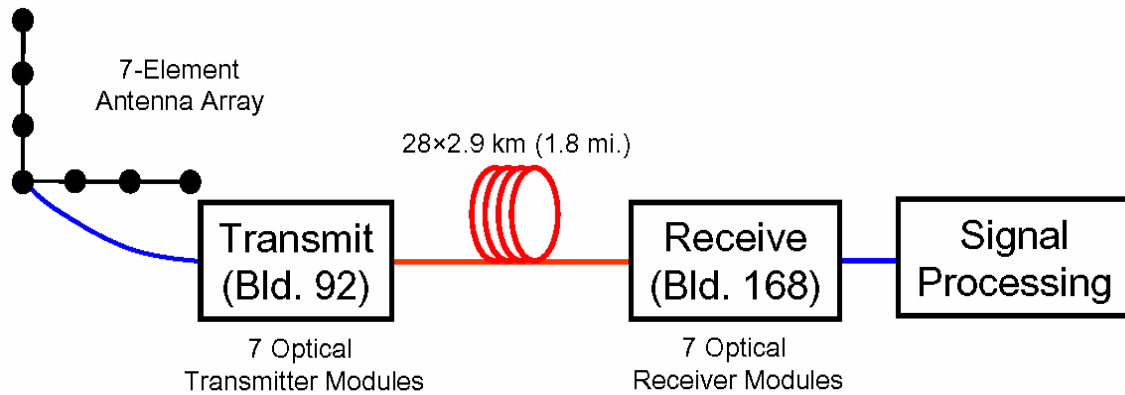


Figure 1. A block diagram for the field test bed, with electrical connections shown in blue and optical connections shown in red. A seven-element “L-array” is electronically connected to seven fiber-optic transmitter modules. Each transmitter has four optical outputs, yielding a 28-fiber run to the seven optical receivers, which are electronically connected to signal-processing hardware.

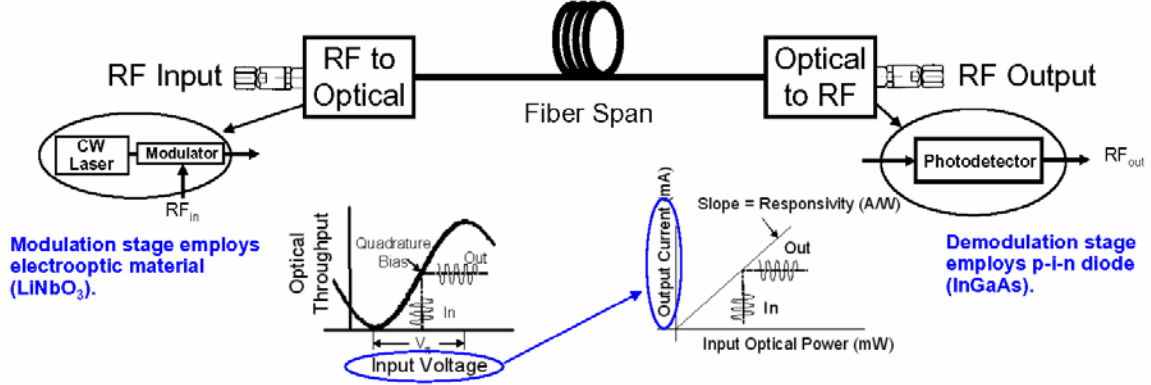


Figure 2. The general concept of an intensity-modulation, direct-detection (IMDD) analog photonic link. A continuous-wave (CW) laser is modulated by a radio-frequency (RF) input to an electrooptic modulator, typically a Mach-Zehnder modulator (MZM). The intensity-modulated light is converted back to an RF current via a photodiode.

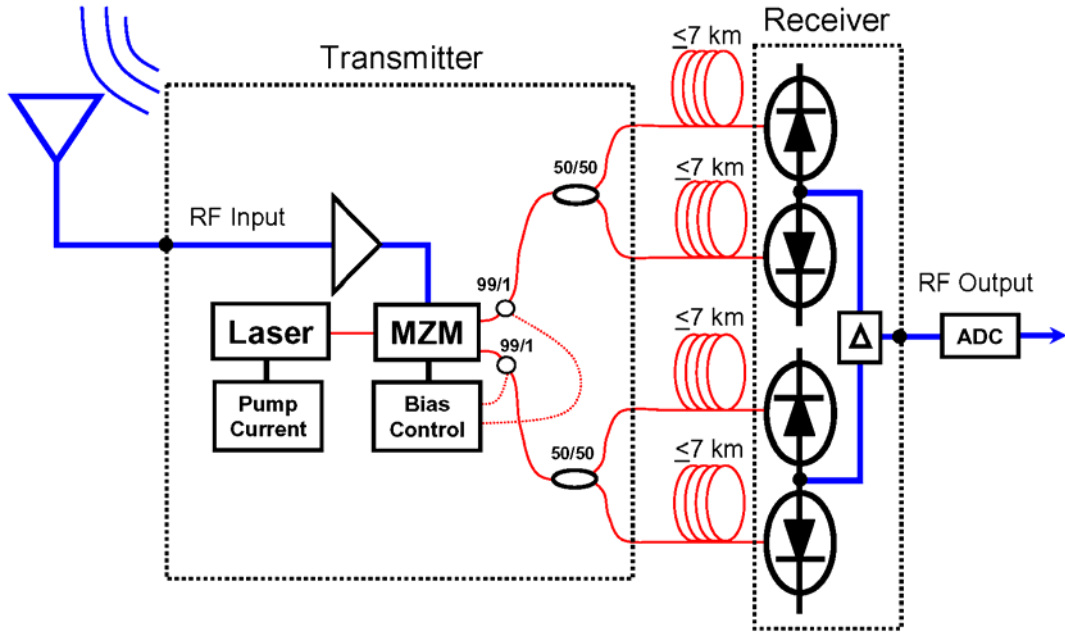
2 LINK DESIGN

A thorough explanation and analysis of the link design is provided in [1]. In this section, the design is reviewed at level appropriate to understand the field test results. The fiber-optic link employs an intensity-modulation, direct detection (IMDD) format where laser light is intensity modulated by the incoming radio-frequency (RF) radiation, propagated through a fiber-optic span and then demodulated back to an RF current with a photodiode. A generic representation of this process is provided in Figure 2. In a typical IMDD architecture, an external electrooptic Mach-Zehnder modulator (MZM) is used for the electrical-to-optical (EO) conversion and a p-i-n photodiode provides the optical-to-electrical (OE) demodulation. The transfer functions for these processes are shown in Figure 2. The fiber-optic link employed in the field test utilizes an IMDD format with some variations to optimize performance.

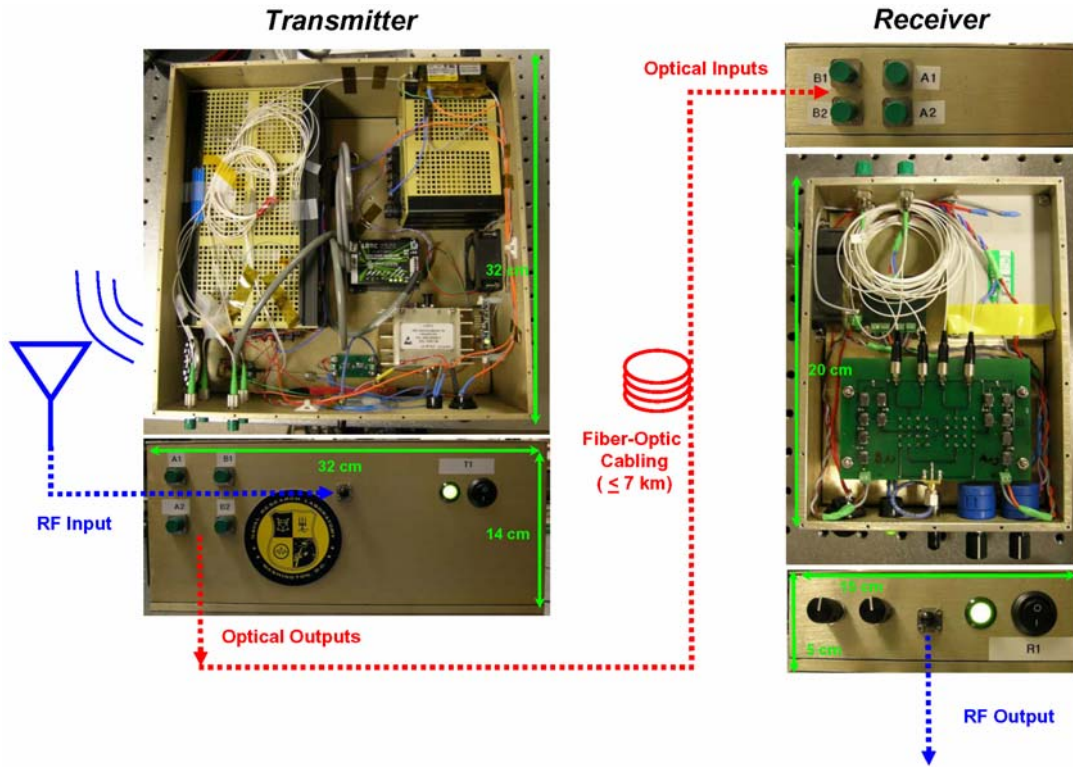
A block diagram for the fiber-optic link is shown in Figure 3(a). For each antenna element there are a transmitter and receiver with four optical fibers connecting them. The four optical fibers allow for optimized performance, mitigating optical fiber nonlinearities such as stimulated Brillouin scattering (SBS), and deliver maximum optical power to the receiver without optical amplification [1]. This link design delivers up to 20 dB more optical power to the user than the most stringent telecommunication links, such as a high-definition television (HDTV) passive optical network (PON) [2]. This increased performance comes at two cabling costs. First, four times the optical fiber is required for this link design. However, a multiple-fiber cable is already required for an antenna array and the cost of adding additional fibers to a fiber-optic cable is negligible compared to the cost of installing the cable. Second, the four fibers per antenna element must be phase matched, which adds installation time. Given the fact that every antenna element must be phase matched to each other, the added time required to phase match an additional three fibers per element is most likely worth the increased performance. A detailed description of the phase matching procedure is given in Section 3.

Though there are four fibers per antenna element, the electrical circuit comprises a single RF input and a single RF output (SMA bulkheads). The transmitter consumes a maximum of 42.5 W of DC power, 12.5 W of which is due to the RF preamplifier that can be bypassed if necessary. The receiver uses 1.2 W of DC power. The total cost per transmitter/receiver pair is about \$12,400 excluding assembly, installation and the cost of the fiber-optic cable (see Appendix II).

As shown in Figure 3(a) the antenna element is connected directly to the RF input on the transmitter, which is followed by the RF amplifier and the EO conversion stage employing a dual-optical-output MZM. One percent of the light on each MZM output is picked off and fed to



(a)



(b)

Figure 3. (a) Block diagram for the fiber-optic link. MZM: Mach-Zehnder modulator, ADC: analog-to-digital converter. (b) Photograph of the transmitter and receiver units with dimensions shown in green. For both (a) and (b) blue designates the radio-frequency (RF) paths and red designates the optical paths.



Figure 4. Clockwise from upper left: 1) Initial fiber fan out showing one of the 12-fiber bundles (green) with all of the bare fiber exposed. Also shown are the FC/APC terminations. 2) A splice tray holding 12 splices from bare fiber to the FC/APC termination. 3) The inside of the fan-out enclosure. 4) The final receiver mounting showing the fan-out enclosure, the FC/APC terminations and the receiver modules. Though not shown here, the terminations connect to the inputs on the receiver modules.

a bias controller, which is used to maintain the proper quadrature bias for the MZM. Each MZM output is then split and fed into the fibers for signal propagation. As shown in Figure 3(b), the four optical outputs on the transmitter are connectorized using FC/APC connections for mating to the fiber-optic cable. The receiver has four FC/APC-terminated optical inputs, which feed to a custom photodiode array that minimizes even-order distortions [1],[3]. The RF output of the receiver feeds an analog-to-digital converter (ADC) or other equipment defined by the user.

3 PREPARATION AND INSTALLATION

This section details the preparation and installation of the link as it was conducted at the field site. Each site will ultimately have its own specific procedures but the steps described below should be general. The phase matching procedure is the most time-consuming and important part of the installation process. Therefore, a more detailed description of the phase-matching process is provided, as compared to, say, the installation of the fiber-optic cable.

The fiber-optic cable employed for this test was a 48-fiber loose-tubing bundle with a length of approximately 2.9 km. The fiber run was installed by the staff at SwRI, with the characterization, termination and phase matching left to the NRL staff. Before phase matching, the cable needed to be fanned out and terminated on one end. Photographs of this procedure are provided in Figure 4. The 48-fiber bundle was subdivided into 4×12 color-coded tubes, with the 12 fibers in an individual tube also color coded. The color coding allows for record keeping during the fan out. After fanning out the individual fibers, a fusion splicer was employed to terminate each fiber *on the receive end only* with FC/APC fiber-optic connectors. Though only 28 fibers are required for the seven-element array, 36 fibers were terminated in order to allow for future upgrades. Once the splicing and organization was completed, optical insertion loss measurements were conducted.

For the insertion loss measurements, a known optical input power was launched into each connectorized fiber from the receive end of the link. On the transmit side of the link, the un-

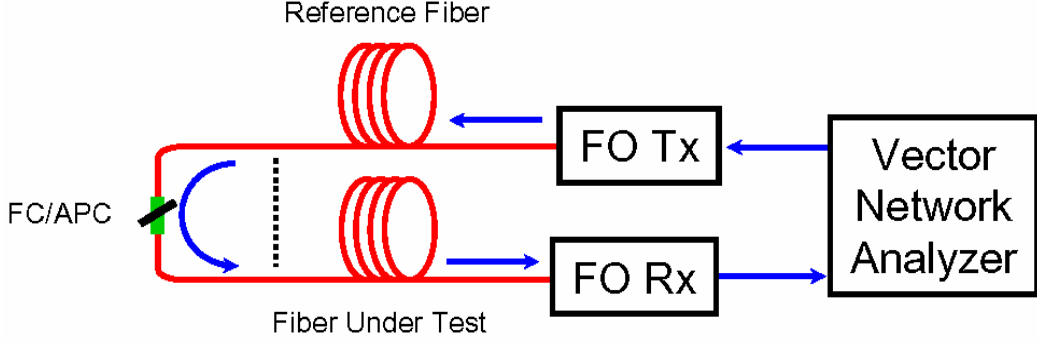


Figure 5. Phase-matching architecture. Red designates optical fiber and blue designates the RF path.

terminated fibers were cleaved and the optical power was measured to determine the insertion loss of the fiber under test. For the 36 fibers, the average optical insertion loss was 0.8 dB with a minimum of 0.5 dB and a maximum of 1.8 dB. Of the 36, the 28 lowest insertion losses were chosen for the field test. Of these 28, the average optical insertion loss was 0.7 dB with a range of 0.5 dB to 0.8 dB. In order to equalize the RF gain, the optical launch powers into the fiber spans were adjusted to compensate for the varying insertion loss of the cable. For example, the laser power for the span with 0.5 dB loss was backed off 0.3 dB to equalize it with the highest insertion loss used, 0.8 dB.

In order for an antenna array to provide true real-time DF, the array must be phase matched. Therefore, each of the fiber-optic links connected to the individual antenna elements must also be phase matched if they are to provide any utility. In addition, each of the four fibers that comprise an individual link must be phase matched to constructively recombine the HF signal after propagation through the optical fiber. It is important to note that the phase matching is tolerant to the HF range, not to optical frequencies. The setup used for phase matching at this installation is shown in Figure 5. The receiver modules were transported to the transmit side of the link, such as to co-locate the transmitters and receivers in order to connect them to a vector network analyzer (VNA). A fixed reference fiber was used and each of the fibers under test was interchanged on the transmit side. The transmitter was modulated with an RF signal from the VNA, which then propagates the reference fiber and fiber under test before being demodulated with the receiver. By measuring phase as a function of frequency with the VNA, the physical length of the fiber can be measured using the relationship

$$L = \frac{\phi_{rf} c}{360 n f_{rf}}, \quad (1)$$

where ϕ_{rf} is the RF phase at frequency f_{rf} , c is the speed of light in vacuum, and $n \cong 1.4682$ is the index of refraction for the fiber. This procedure does not give the length of any fiber under test because the length of the reference fiber is unknown. However, the relative difference of all the test fibers is obtained with this approach. Once all fibers have been measured, the 27 longest fibers are trimmed back to equal the length of the shortest remaining fiber. For the fiber in this field test it was determined that the longest relative difference was 4.1 m, about 0.14% of the total length of the cable. Luckily, there was enough fiber exposed from the installation to cut 4.1 m from the longest length. Care must be taken to ensure that enough fiber is exposed to complete the phase matching. Phase matching the cable before it is installed can mitigate this issue. The accuracy to which the cables must be trimmed is a function of the tolerable phase error. Differentiating Equation (1) yields the phase error as a function of length difference:

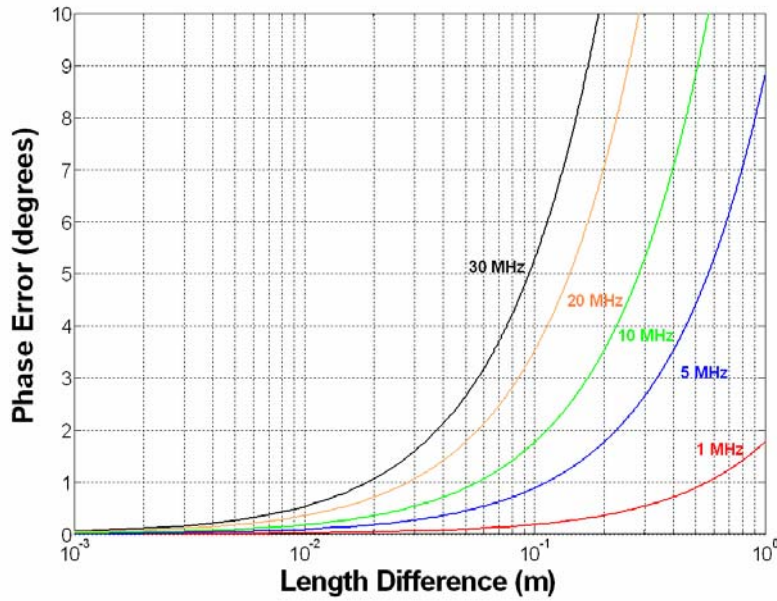


Figure 6. Calculated phase error as a function of length difference and frequency as given by Equation (2).

$$d\phi_{\text{rf}} = \frac{360nf_{\text{rf}}}{c} dL. \quad (2)$$

Equation (2) is plotted in Figure 6, demonstrating that for 1° maximum phase error across the HF band, all fibers must be within about 1.9 cm of each other. The maximum allowable difference for this field test was set at 1.5 cm including the terminations and transmitter and receiver modules, which according to Equation (2) gives a 0.8° relative phase error at 30 MHz.

Other techniques for phase matching are certainly possible, such as pulsed RF approaches, as long as the required resolution is maintained. An alternative phase-matching approach is shown in Figure 7. A fiber-coupled Faraday-rotation mirror (FRM) can be connected to one side of the fiber under test where the other side is connected to a fiber-optic circulator followed by the transmitter and receiver modules. In this configuration the phase as a function of frequency is measured just as above and the absolute length of each fiber is obtained. The absolute length of the fiber under test is more easily obtained using this method as compared to the technique described above. (The absolute length can be obtained with the method above if the reference fiber is measured with respect to two phase-matched fibers, albeit with less accuracy.) Regardless of the technique, the phase matching is a procedure that must be completed carefully because failure to do so will result in phase errors. However, as described in [1], the phase-matching process must be completed only once. That is, the fiber at these lengths will remain stable in terms of phase errors in the HF band.

Once the phase matching was completed and the transmitter side of the link was terminated, all of the receiver modules were transported back the receive end of the link. As shown in Figure 8, the transmitter modules took up the better part of an equipment rack. For indoor applications where the antennas are routed to the fiber-optic transmitters, some size reduction is certainly possible. The transmitter modules were individually packaged to allow for versatility in the field test. For example, the individual transmitters could be connected directly to the feed at the base of the antennas with proper environmental enclosures. The receiver modules will in most cases be co-located and the modularization provided here may be not necessary in future deployments.

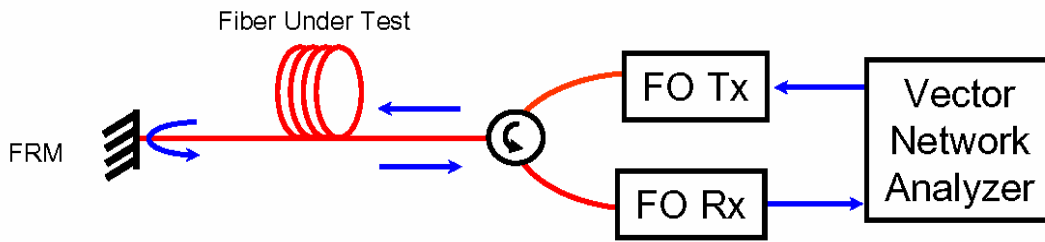


Figure 7. An alternative method to phase match the fiber-optic links using a fiber-coupled Faraday-rotation mirror (FRM) and an optical circulator.



Figure 8. Photographs of the seven fiber-optic transmitters and receivers after being mounted in standard equipment racks. The transmitters are shown with the RF inputs connected. The RF outputs on the receivers are on the back side of the rack and are not connected in the photograph.

4 HF PERFORMANCE

The field test results are shown on Pages 10 and 11. With calibrated RF sources connected to the links, the RF performance metrics of gain (G_{rf}), noise figure (NF_{rf}), compression dynamic range (CDR), and spurious-free dynamic range (SFDR) were measured. The gain and phase stability of the fiber-optic links were also measured. When connected to the antenna array, check targets were measured in order to demonstrate accurate DF capability. The two main results of these tests are that the RF performance metrics measured in the field agree with the previous laboratory results and that accurate direction finding was demonstrated.

In order to characterize the fiber-optic link itself, the RF preamplifier was disconnected and calibrated RF sources were connected directly to the MZM. As shown in Figure 9(a), a two-tone test was conducted at the center frequencies listed in Table 1. Because of limited time at the field test facility, three SFDR measurements were completed. At 22 MHz a SFDR = 117 dB·Hz^{2/3} was measured, reducing to 108 dB·Hz^{2/3} at 2.5 MHz. The SFDR reduction is due to rise in the noise power and not a reduction in linearity. Also, the link was determined to be third-order limited across the band, noting that MZM bias drift may give rise to increased even-order distortion. A manual adjustment is necessary in the bias controllers for these links but plans are underway to include an automated adjustment in next-generation links. With a single tone excitation of the link, the CDR and G_{rf} were also measured with the results shown in Table 1. The G_{rf} was approximately -1 dB across the band and CDR = 169 dB·Hz at the top of the band, dropping to 155 dB·Hz at 2.5 MHz. Again, the reduction in CDR is due to an increased noise floor and not a decreased compression point. The 1-dB compression point for the link was measured as 15 dBm at 2.5 MHz and 13 dBm at 29 MHz. The results in Table 1 are for a single fiber-optic link and it was determined that all of the links had about the same RF performance. A 1×8 multicoupler and an HFX-2000 ADC were used to measure the gain and phase stability from link to link (see Figure 9(b)). The gain equalization at a particular frequency was measured as ±0.5 dB and the maximum phase deviation was 1° at 30 MHz. There was an observed gain and phase ripple near 15 MHz due to the MZM. However, this ripple was stable enough to calibrate out of the DF system and is being addressed by the MZM manufacturer for future applications.

The results from the field test should be compared to the proof-of-principle results in [1]. In Table 2 on Page 19 of [1], the following values were reported for the optics-only portion of the link: $G_{rf} = -0.86$ dB, $NF_{rf} = 21$ dB and SFDR = 116.7 dB·Hz^{2/3}. The CDR was not reported in [1] because it is typically the SFDR that is the limiting dynamic range in fiber-optic links. Comparing these results to those in Table 1 of this report, there is very good agreement over the HF band in terms of G_{rf} and at the top of the band for NF_{rf} and SFDR. The decreased SFDR and increased NF_{rf} at the low end of the band is due to increased electrical noise in the transmitter and receiver modules and environmental noise in the field, as compared to the prototype system on a bench.

The setup for the noise figure measurement and additional noise figure results are shown in Figures 10 and 11, respectively. The noise figures for the transmitter and receiver modules were measured at NRL upon their completion before shipping them to the field site. As mentioned previously, the increased noise at lower frequencies is due to increased electrical noise in the AC-powered modules as compared to the bench-level demonstrations in [1]. There is an additional rise in the low-frequency noise figure in the field and this is attributed to increased environmental noise as compared to the laboratory at NRL. The noise figure with the RF preamplifier is also shown because it will be required in antenna arrays with passive antenna front ends.

With the initial testing and calibrations completed, the fiber-optic links were connected to the antenna array for DF testing. In these tests, the RF preamplifiers in the transmitter modules were bypassed and on-site amplifiers at the antenna bases were employed. The antennas were seven 10-foot Shakespeare whips configured in an “L” array. The DF results are given in Table 2 demonstrating accurate measured bearings. The statistics in Table 2 are for an average of ten collections with the HFX-2000 ADC system.

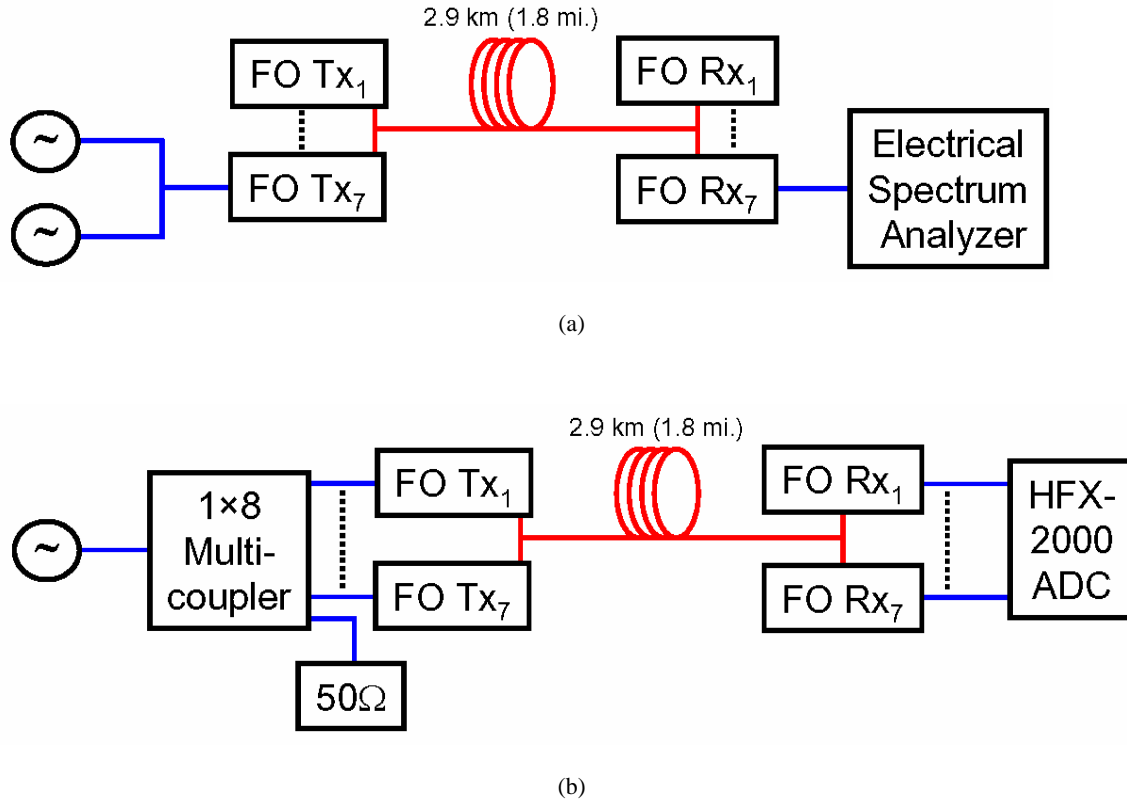


Figure 9. (a) Architecture for measuring the analog performance metrics for one of the fiber-optic links. (b) Setup for measuring gain and phase stability for the array of fiber-optic links. Blue shows the RF paths; red shows the optical paths.

Table 1: Measured Analog Performance Metrics for One of the Fiber-Optic Links

Freq. (MHz)	Gain (dB)	Noise Figure (dB)	CDR (dB-Hz)	SFDR (dB-Hz ^{2/3})
2.5	-0.8	36	155	108
7.5	-0.8	33	not meas.	not meas.
15	-0.1	26	not meas.	113
22	-1.4	20	not meas.	117
29	-1.6	21	169	not meas.

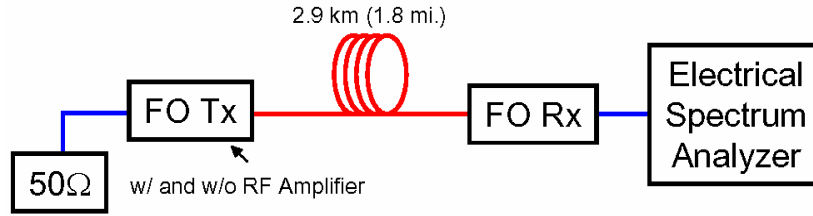


Figure 10. Setup for noise figure measurements. Blue shows the RF paths; red shows the optical paths.

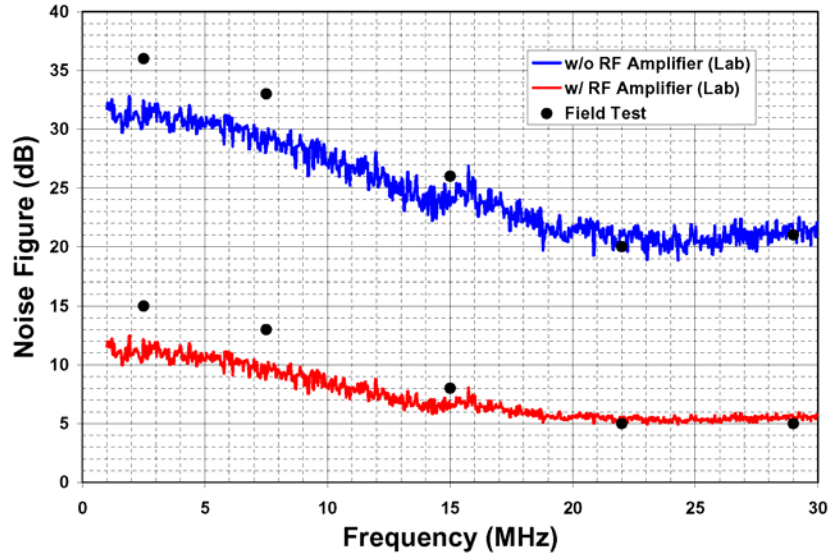


Figure 11. Measured noise figure results in the field (black circles) as compared to laboratory data for both with (red) and without (blue) the RF preamplifier in the fiber-optic transmitter.

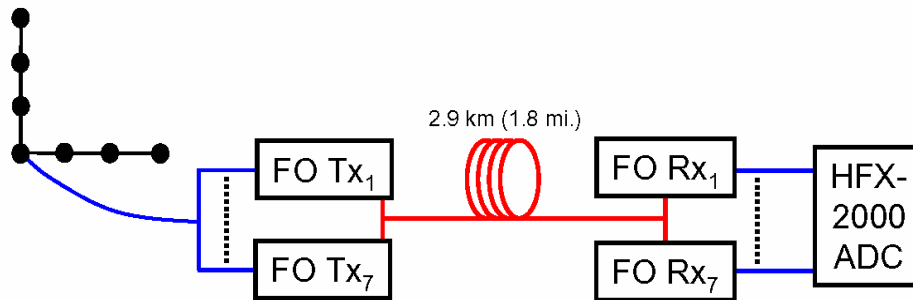


Figure 12. Architecture for direction-finding measurements. Blue shows the RF paths; red shows the optical paths.

Table 2: Measured Results for Direction-Finding Experiments

Check Target	Freq. (MHz)	Known Bearing (Deg.)	Avg. Measured Bearing (Deg.)	Standard Deviation (Deg.)
WWV, Fort Collins, Colorado	10.0000	336.5	339.3	0.2
FUF, Martinique, Caribbean	13.0312	105.5	105.0	0.6
CHU, Ottawa, Canada	14.6700	42.2	43.0	0.9

5 SUMMARY AND CONCLUSIONS

The field test of a 2.9 km fiber-optic link has been successfully completed. Previous results demonstrate that the link provides the same performance up to a distance of 7 km. The installation process of the link has been described, specifically noting that phase matching of the link must be performed. A complete technical report on the link design and proof-of-concept experiments is provided in [1], with a more-detailed description of the novel fiber-optic receiver provided in [3]. The primary results of this report are that the RF performance metrics measured in the field agree with those reported in [1] and that accurate direction-finding capability has been demonstrated. As this report is completed, the links have been in operation for approximately 3.5 months with no reported problems. The units will remain at the Southwest Research Institute for continued use and evaluation.

The remoting of HF antenna with analog fiber-optic links is therefore feasible for distances up to 7 km. Future work on links of these distances includes ruggedization of the transmitter and perhaps the receiver modules, improving the modulator bias controller, and addressing the phase distortions in the modulator near 15 MHz. For this field test and the present application, these issues do not present an obstacle.

Future work in the field of HF photonics will be centered on increasing the distance to 100 km, and perhaps as long as 1000 km, without compromising performance. This is no small task and will require research and development in various areas. In addition to NRL's general experience in long-haul analog photonics [4]-[6], previous work at NRL on microwave photonics can be applied to the HF range to extend the transmission distance. These research areas include, but are not limited to, novel analog-photonics modulation formats [7]-[11], optical amplifiers for analog signals [12]-[14], and analog wavelength-division multiplexing (WDM) [15]-[21]. Leveraging this work and applying it to the HF range will open new avenues of applied research on ultra-long-haul HF links. Therefore, the field of HF photonics and its applications has just started to grow.

ACKNOWLEDGEMENTS

The authors wish to acknowledge the exceptional support and hospitality provided by the Signal Exploitation and Geolocation Division at the Southwest Research Institute (SwRI). Don Fritz allowed access to all of his resources, allowing for a successful field test. Patrick Siemsen provided his expertise in analog electronics and executed a test plan for verification of performance. In particular, we acknowledge Hervey "Slim" Lefrere and Carl Zigmond for their continuous and courteous support during the field test. Carl and Slim shared their expertise in SwRI's systems without hesitation or reservation; without them, the operation would not have run as smoothly as it did.

REFERENCES

- [1] V. J. Urick, J. Diehl, A. Hastings, C. Sunderman, J. D. McKinney, P. S. Devgan, J. L. Dexter, and K. J. Williams, "Analysis of fiber-optic links for HF antenna remoting," NRL Memorandum Report, NRL/MR/5650-08-9101, Mar. 2008.
- [2] R. E. Wagner, J. R. Igel, R. Whitman, M. D. Vaughn, A. B. Ruffin, and S. Bickham, "Fiber-based broadband-access deployment in the United States," *J. Lightwave Technol.*, vol. 24, no. 12, pp. 4526-4540, Dec. 2006.
- [3] A. S. Hastings, V. J. Urick, C. Sunderman, J. F. Diehl, J. D. McKinney, D. A. Tulchinsky, P. S. Devgan, and K. J. Williams, "Suppression of even-order photodiode nonlinearities in multi-octave photonic links," accepted for publication in *J. Lightwave Technol.*, 2008.
- [4] A. J. Seeds and K. J. Williams, "Microwave photonics," *J. Lightwave Technol.*, vol. 24, no. 12, pp. 4628-4641, Dec. 2006.
- [5] E. E. Funk, V. J. Urick, and F. Bucholtz, "High dynamic range, long haul (>100 km) radio over fiber," in *Microwave Photonics*, C. H. Lee (editor), CRC Press, Ch. 6, pp. 185-212, 2007.
- [6] V. J. Urick, "Long-haul analog photonics principles with applications," Doctoral Dissertation, UMI No. 3255815, 2007.
- [7] V. J. Urick, M. S. Rogge, P. F. Knapp, L. Swingen, and F. Bucholtz, "Wideband predistortion linearization for externally-modulated long-haul analog fiber optic-links," *IEEE Trans. Microwave Theory Tech.*, vol. 54, no. 4, pp. 1458-1463, Apr. 2006.
- [8] A. L. Campillo and F. Bucholtz, "Chromatic dispersion effects in analog polarization-modulated links," *Appl. Opt.*, vol. 45, no. 12, pp. 2742-2748, Apr. 2006.
- [9] V. J. Urick, M. S. Rogge, F. Bucholtz, and K. J. Williams, "Wideband (0.045-6.25 GHz) 40-km analog fiber-optic link with ultra-high (>40 dB) all-photonic gain," *Electron. Lett.*, vol. 42, no. 9, pp. 71-72, Apr. 2006.
- [10] V. J. Urick, F. Bucholtz, P. S. Devgan, J. D. McKinney, and K. J. Williams, "Phase modulation with interferometric detection as an alternative to intensity modulation with direct detection for analog-photonic links," *IEEE Trans. Microwave Theory Tech.*, vol. 55, no. 9, pp. 1978-1985, Sept. 2007.
- [11] B. M. Haas, V. J. Urick, J. D. McKinney, and T. E. Murphy, "Dual-wavelength linearization of optically phase-modulated analog microwave signals," accepted for publication in *J. Lightwave Technol.*, 2008.
- [12] V. J. Urick, F. Bucholtz, and K. J. Williams, "Optically-amplified short-length analog photonic links," *IEEE Topical Meeting on Microwave Photonics*, Grenoble, France, paper W2.2, Oct. 2006.
- [13] V. J. Urick, M. S. Rogge, F. Bucholtz, and K. J. Williams, "The performance of analog photonics links employing highly-compressed erbium-doped fiber amplifiers," *IEEE Trans. Microwave Theory Tech.*, vol. 54, no. 7, pp. 3141-3145, July 2006.
- [14] P. S. Devgan, V. J. Urick, J. D. McKinney, and K. J. Williams, "Cascaded noise penalty for amplified long-haul analog fiber-optic links," *IEEE Trans. Microwave Theory Tech.*, vol. 55, no. 9, pp. 1973-1977, Sept. 2007.
- [15] A. L. Campillo, E. E. Funk, D. A. Tulchinsky, J. L. Dexter, and K. J. Williams, "Phase performance of an eight-channel wavelength-division-multiplexed analog delay line," *J. Lightwave Technol.*, vol. 22, no. 2, pp. 440-447, Feb. 2004.
- [16] F. Bucholtz, V. J. Urick, and A. L. Campillo, "Comparison of crosstalk for amplitude and phase modulation in an analog fiber optic link," in *IEEE Topical Meeting on Microwave Photonics*, Ogunquit, pp. 66-69, Oct. 2004.
- [17] M. S. Rogge, V. J. Urick, F. Bucholtz, K. J. Williams, and P. Knapp, "Comparison of amplitude and phase modulation crosstalk in hyperfine WDM fiber optic links," in *CLEO Technical Digest*, Baltimore, paper CMH2, May 2005.

- [18] A. L. Campillo, "Interchannel nonlinear crosstalk in analog polarization modulated WDM systems," *J. Lightwave Technol.*, vol. 24, no. 3, pp. 1186-1193, Mar. 2006.
- [19] B. S. Marks, C. R. Menyuk, A. L. Campillo, and F. Bucholtz, "Analysis of interchannel crosstalk in a dispersion-managed analog transmission link," *J. Lightwave Technol.*, vol. 24, no. 6, pp. 2305-2310, June 2006.
- [20] A. L. Campillo and F. Bucholtz, "Increased nonlinear crosstalk in analog wavelength-division-multiplexed links due to the chromatic dispersion of optical filters," *IEEE Photon. Technol. Lett.*, vol. 19, no. 19, pp. 2014-2016, Oct. 2006.
- [21] B. S. Marks, C. R. Menyuk, A. L. Campillo, and F. Bucholtz, "Interchannel crosstalk reduction in an analog fiber link using dispersion management," *IEEE Photon. Technol. Lett.*, vol. 20, no. 4, pp. 267-269, Feb. 2008.

APPENDIX I: BASIC OPERATING INSTRUCTIONS

The basic operating instructions for the fiber-optic links are given in terms of power-up and power-down procedures. One of the authors of this report should be consulted for detailed adjustments inside of the transmitter/receiver enclosures. While mean time between failure (MTBF) calculations have yet to be completed for the link, it was intended to run continuously after the installation. The fiber-optic connectors should not be removed. If they are, proper cleaning is required to maintain system performance. Under no circumstances should the fiber-optic connectors be removed while the fiber-optic transmitters are on, as non-visible laser radiation will be emitted.

Turn-On Procedure

- Load the RF output on the fiber-optic receivers.
- Turn on power to the fiber-optic receivers.
- Turn on power to the fiber-optic transmitters.
- Attach RF connections to the fiber-optic transmitters.

Turn-Off Procedure

- Disconnect RF connections to the fiber-optic transmitters.
- Turn off power to the fiber-optic transmitters.
- Turn off power to the fiber-optic receivers.
- Disconnect RF connections to the fiber-optic receivers.

Direct all inquires to:

Dr. Vincent J. Urick
U.S. Naval Research Laboratory
Code 5650: Photonics Technology
4555 Overlook Ave. SW
Washington, DC 20375
phone: 202-767-9352
fax: 202-404-8645
email: vincent.urick@nrl.navy.mil

APPENDIX II: PARTS LIST

Shown below in Table 3 are the part costs, as sold to NRL, for the components comprising the fiber-optic transmitter and receiver. The initial NRE, the fiber-optic cable installation, and the cost to assemble, test and install the units are not included.

Table 3: Part Costs for Fiber-Optic Transmit and Receive Modules

TRANSMITTER					
Part	Vendor	Vendor Part #	Cost Per	Quantity	Total Cost
Dual Output MZM	EO Space	AZ-1x2-0K5-10-PFU-SFU-UL	\$4,990	1	\$4,990
RF Amplifier	AML	AR01003251X	\$1,908	1	\$1,908
DFB Laser	EM4	EM253-080-YY3	\$1,800	1	\$1,800
Bias Control Board	YY Labs	Ditherless Bias Controller	\$875	1	\$875
Shielded Box	Compac	S71212-500-0	\$428	1	\$428
Laser Driver	Wavelength Electronics	LDT0520	\$371	1	\$371
12 V Power Supply	Acopian	TD12-250	\$270	1	\$270
Fiber Optic Patch Cable	Textron	2828-901-2	\$70	2	\$140
30 V Power Supply	Acopian	B30GT50	\$115	1	\$115
50/50 Coupler	JDSU	JDSU FFC-CK32PB110	\$55	2	\$110
99/1 Coupler	Gould	440-000047	\$55	2	\$110
FC/APC Bulkhead	Textron	MPC-108	\$16	4	\$64
Filter Circuit	Colonial Circuits/NRL	1101.LCFILTER	\$50	1	\$50
SMA Cable	Astrolab	Minibend 6	\$20	2	\$40
SMA Bulkhead	Astrolab	29074F-1	\$37	1	\$37
Fan	Digikey	259-1429-ND	\$21	1	\$21
AC Receptacle	Digikey	CCM1000-ND	\$20	1	\$20
Voltage Regulator	Digikey	LT-323AT-ND	\$4	1	\$4
Switch	Digikey	EG-4564-ND	\$3	1	\$3
Fan Guard	Digikey	FG-5 50MM FINGER GUARD-ND	\$1	2	\$2
Fuse	Digikey	283-2022-ND	\$1	1	\$1
LED	Digikey	67-1172-ND	\$1	1	\$1
					\$11,360
RECEIVER					
Part	Vendor	Vendor Part #	Cost Per	Quantity	Total Cost
Combiner Board	Colonial Circuits/NRL	1101.HFRECEIVER	\$300	1	\$300
Shielded Box	Compac	S58060-175-0/WU9170	\$300	1	\$300
Photodetectors	Applied Optoelectronics, Inc.	PD1000-FA-10-H-B	\$25	4	\$100
Power Supply	Acopian	D12-10A	\$75	1	\$75
FC/APC Bulkhead	Textron	MPC-108	\$16	4	\$64
Power Conditioning Board	Colonial Circuits/NRL	1101.POWERSUPPLY	\$50	1	\$50
SMA Bulkhead	Astrolab	29074F-1	\$37	1	\$37
AC Receptacle	Digikey	CCM1000-ND	\$20	1	\$20
Potentiometers	Digikey	3590S-2-502L-ND	\$10	2	\$20
SMA Cable	Astrolab	Minibend 6	\$20	1	\$20
Knob	Digikey	226-4041-ND	\$5	2	\$10
Switch	Digikey	EG-4564-ND	\$3	1	\$3
LED	Digikey	67-1172-ND	\$1	1	\$1
Fuse	Digikey	283-2009-ND	\$0	1	\$0
					\$1,001
				Tx/Rx	\$12,361

